Track changes is off Everyone Track changes for everyone vmgub Track changes for vmgub You Track changes for You Guests Track changes for guests Current file Overview 32

Interference-enhanced absorption of visible and near-infrared radiation in ultrathin film coatings

V. Medvedev, V. Gubarev, E. Zoethout, N. Novikova,

We report the interference-enhanced absorption of electromagnetic radiation in two-layer lossy coatings on metal substrates. The conditions for the complete absorption of monochromatic radiation are described in comparison with those in previously studied single-layer coatings. Proof-of-principle measurements of the interference-enhanced absorption in the near-infrared range are presented for silicon-on-germanium coatings on aluminum substrates. We also provide various examples of materials that can be used to create similar light-absorbing coatings for visible and near-infrared ranges. The proposed design can be applied to optical filters, optoelectronic devices, photodetectors, and light-emitting devices.

***Index Terms*—tuning electromagnetic wave absorption, ultrathin film, optical reflection.**

I. Introduction

The phenomenon of interference is a powerful tool for manipulating the interaction of electromagnetic radiation with matter. Interference allows controlling absorption and reflection properties of radiation in materials. This is of great importance for numerous applications such as photovoltaics, biosensing, light detection, thermal imaging, radiative cooling, and efficient light emission.

Interference-enhanced absorption in stratified media has been studied since the 1930s [1], [2], [3], [4], [5]. However, in recent years, a new wave of interest has emerged in this research topic [6], [7], [8], [9], [10], [11], [12]. Among the new works, it is worth highlighting the paper by Kats et al. on the absorption of light in ultrathin semiconductor layers on a metal substrate [6]. These authors showed that strong absorption can be achieved in a layer of a lossy material with an optical thickness substantially lower than a quarter of the wavelength of the incident radiation. Park et al. later derived the conditions of unit absorption at a target wavelength for such structures. They showed that this remarkably high absorption occurred because of the coupling of the incident light to the surface mode supported in a single-layer coating [13], [14]. This surface mode has flat dispersion in both the transverse electric and magnetic polarization states, which results in omnidirectional and polarization-independent absorption. Importantly, such a single-layer coating allows the complete absorption of incident radiation at only one unique wavelength. This unity-absorption wavelength is determined by the optimal matching of the complex refractive indices of substrate and coating materials. With a change in the wavelength, this matching is violated because of the dispersion of the optical constants of the materials and, as a result, the interference is unable to suppress the reflection completely. By varying the combination of the coating and substrate materials, the unity-absorption wavelength can be changed in discrete steps. However, it is fundamentally interesting to find ways to change this wavelength continuously or to achieve complete absorption at an arbitrarily given wavelength from a certain spectral range. As one way, Park et al. suggested replacing the planar metal substrate with a metal metasurface substrate [15]. Such a metasurface in the form of a subwavelength metal grating allows tailoring the reflective properties of the interface between a lossy coating and a substrate. In another method, Kats et al. suggested using phase-changing materials for the coating, i.e., materials that change the optical constants upon heating [16]. In this case, controlled heating of the coating structure allows varying the position of the interference absorption peak within a certain spectral range. Other studies have described a combination of both approaches when phase-changing materials are integrated into light-absorbing metasurfaces [17], [18], [19].

In this study, we investigate the optical absorption in two-layer lossy coatings on metal substrates. Such coatings can be composed of various lossy dielectric or semiconductor materials. Both coating materials A and B, in combination with substrate material M, determine the unity absorption wavelengths $\lambda_0^{A/M}$ and $\lambda_0^{B/M}$, corresponding to A/M and B/M single-layer coatings. We show that two-layer A/B/M and B/A/M coatings enable the complete absorption of normally incident monochromatic radiation of any wavelength from the spectral range limited by the values of $\lambda_0^{A/M}$ and $\lambda_0^{B/M}$. For each target wavelength, this was achieved by optimizing the thickness of the coating layer. It is important to emphasize that the total thickness of the optimized coating layers does not exceed a quarter of the target wavelength. Using numerical calculations, we analyzed in detail the absorption of near-infrared radiation in coatings based on a combination of Si and Ge layers on an Al substrate. The results of these calculations are complemented with an experimental demonstration of the interference-enhanced absorption in Si/Ge/Al layered systems. In addition, we discuss other combinations of materials that can be used to produce coatings for visible and near-infrared radiation.

V. Medvedev and V. Gubarev were with Institute of Spectroscopy of the Russian Academy of Science, Troitsk, Moscow 108840, Russia; and Moscow Institute of Physics and Technology (State University), Dolgoprudny, Moscow region 141701, Russia, e-mail: medvedev@phystech.edu

E. Zoethout was with Dutch Institute for Fundamental Energy Research, Eindhoven 5612, Netherlands

N. Novikova was with Institute of Spectroscopy of the Russian Academy of Science, Troitsk, Moscow 108840, Russia

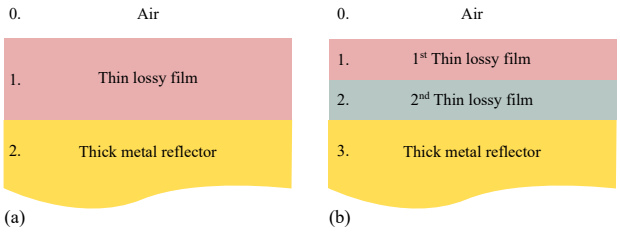

Fig. 1. (a) Sketch of a single-layer lossy coating on a metal substrate. (b) Sketch of a two-layer lossy coating on a metal substrate.

II. Conditions for unity absorption

Consider the interaction of a normally incident plane electromagnetic wave with a single-layer and two-layer coating, as shown in Fig. 1. For this purpose, we use the partial-wave interference formalism. Because the considered structures have opaque metal substrates, the absorption coefficient is defined as $A = 1 - R = 1 - |r|^2$, where r and R stand for the amplitude and intensity reflection coefficients, respectively. The amplitude reflection coefficient of the single-layer coating r_{1L} can be written as the superposition of the partial wave directly reflected from the first interface (with the reflection coefficient $r_0 = r_{01}$) and the partial waves reflected after m circulations inside the layer (with the reflection coefficients $r_m = t_{01}t_{10}r_{12}^m r_{10}^{m-1}\exp(2mik_1d_1)$):

$$r_{1L} = \sum_{m=0}^{\infty} r_m = r_{01} + \frac{t_{01}t_{10}}{r_{10}} \sum_{m=1}^{\infty} (r_{12}r_{10}\exp(2ik_1d_1))^m. \quad (1)$$

In Eq. 1, r_{pq} and t_{pq} represent the Fresnel coefficients for a plane wave that encounters medium q from medium p. The media are numbered as shown in Fig. 1. Using the well-known relations for the Fresnel coefficients and the formula for the sum of a series of geometric progressions, one can change Eq. 1 to the following form:

$$r_{1L} = \frac{r_{01} + r_{12}\exp(2ik_1d_1)}{1 + r_{01}r_{12}\exp(2ik_1d_1)}. \quad (2)$$

Similarly, one can write an expression for the amplitude reflection coefficient of the two-layer coating r_{2L} through the coherent sum of the partial waves:

$$r_{2L} = \sum_{m=0}^{\infty} r_m = r_{01} + \frac{t_{01}t_{10}}{r_{10}} \sum_{m=1}^{\infty} (r_{123}r_{10}\exp(2ik_1d_1))^m, \quad (3)$$

where the coefficient r_{123} is expressed by Eq. 4, considering the propagation and interference of the partial waves in the bottom layer of the coating.

$$r_{123} = \frac{r_{12} + r_{22}\exp(2ik_2d_2)}{1 + r_{12}r_{23}\exp(2ik_2d_2)}. \quad (4)$$

Eq. 3 can also be reduced to the following simpler form:

$$r_{2L} = \frac{r_{01} + r_{123}\exp(2ik_1d_1)}{1 + r_{01}r_{123}\exp(2ik_1d_1)}. \quad (5)$$

First, we briefly review the reflection and absorption properties of single-layer coatings. Owing to the interference of waves reflected from the upper and lower coating interfaces, the reflection coefficient $R = |r_{1L}|^2$ at a wavelength λ is an oscillating function of the thickness d_1. Ultrathin absorber coatings make use of the first interference minimum of the reflection coefficient, R_{min}, corresponding to the minimum thickness $d_{1,min}$. For an arbitrary wavelength, R_{min} and $d_{1,min}$ can be calculated by applying a numerical optimization routine, e.g., the Nelder–Mead minimization algorithm. Consider, as an example, a Si coating on an Al substrate. The optical constants of Si and Al were obtained from Refs. [20], [21]. A numerical analysis of the dependence of R_{min} on λ for such a system shows that R_{min} becomes zero (within the computer precision) at wavelengths of $\lambda_0^{Si/Al} \approx 627$ nm, which is the unity absorption wavelength for Si/Al coatings. The corresponding optimal thickness of the Si layer is $d_{1,min} \approx 26$ nm, which is equal to an optical thickness of 0.175λ. Let us now consider a Ge coating on an Al substrate. The optical constants of Ge were obtained from Refs. [22]. A similar numerical analysis shows that the unity absorption wavelength for a Ge/Si coating is $\lambda_0^{Ge/Al} \approx 1001$ nm, and the corresponding optimal Ge layer thickness is $d_{1,min} \approx 38$ nm (0.18λ).

What happens if Si and Ge layers are combined on an Al substrate? In the case of a two-layer coating, one can apply numerical optimization routines to search for the value R_{min} representing the reflection coefficient for the first interference minimum. First, we consider coatings with a Si layer on top of a Ge layer. Fig. 2(a) shows the calculated dependence of R_{min} on λ for such a Si/Ge/Al coating. Note that each point on this curve represents a unique coating structure with layer thicknesses $d_{1,min}$ and $d_{2,min}$ corresponding to the first interference minimum of reflection. Fig. 2(b) plots $d_{1,min}$ and $d_{2,min}$ versus λ. The vertical dotted lines in Fig. 2 denote the positions of the unity absorption wavelengths for the single-layer Si/Al and Ge/Al coatings. The Si/Ge/Al coatings allow zero reflection (unity absorption) for any wavelength in the spectral range between the wavelengths corresponding to the single-layer coatings. The coating composition gradually changed from pure Si (i.e., $d_{2,min} = 0$) at $\lambda = \lambda_0^{Si/Al}$ to pure Ge (i.e., $d_{1,min} = 0$) at $\lambda = \lambda_0^{Ge/Al}$. It is also worth mentioning that the net optical thickness of the Si/Ge/Al coating $(n_1d_{1,min} + n_2d_{2,min})$ does not exceed 0.2λ in this spectral range. The calculation results for two-layer coatings with a Ge layer on top of a Si layer are similar. In particular, Ge/Si/Al coatings also allow unity absorption at any wavelength in the range from $\lambda_0^{Si/Al}$ to $\lambda_0^{Ge/Al}$. The only difference between these coatings is in the optimal layer thickness.

To explain the results presented in Fig. 2a, we compare the reflection from single-layer and two-layer structures in terms of the interference of the partially reflected waves expressed by Eqs. 1 and 3 using the phasor diagram technique. Fig. 3a and 3b show the calculated phasor diagrams for the reflection of the single-layer Si/Al and Ge/Al coatings under the conditions when unity absorption is realized at the wavelengths $\lambda_0^{Si/Al}$ and $\lambda_0^{Ge/Al}$, respectively. The phasor trajectories return to their origin in the cases corresponding to zero reflection. Subsequently, we choose an arbitrary value in between these "resonant" wavelengths, e.g., $\lambda = 800$ nm. At

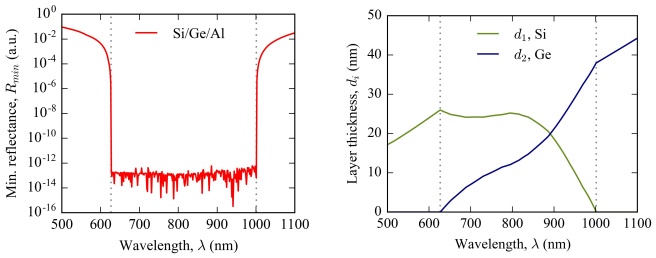

a) b)

Fig. 2. (a) Calculated dependence R_{min} on λ for Si/Ge/Al coatings. (b) Calculated dependencies $d_{1,min}$ on λ (green curve) and $d_{2,min}$ on λ (blue curve) for Si/Ge/Al coatings. Vertical gray lines denote the unity absorption wavelength for Si/Al and Ge/Al coatings: $\lambda_0^{Si/Al} \approx 627$ nm and $\lambda_0^{Ge/Al} \approx 1001$ nm.

this wavelength, a Si/Al coating with a Si layer thickness of $d_{1,min} \approx 39$ nm achieves a minimum reflection coefficient of $R_{min} \approx 0.05$. Fig. 3c shows the calculated phasor diagram for the reflection at $\lambda = 800$ nm for such a structure. As can be seen, a relatively low extinction coefficient of Si at this specified wavelength does not provide sufficient attenuation of the partial waves circulating in the coating layer for unity absorption. In the case of the Ge/Al coating, the opposite is true: the extinction coefficient of Ge is larger than that required to provide sufficient attenuation of the partial waves. This can be seen from Fig. 3d that shows the calculated phasor diagram for the reflection of the Ge/Si coating at the same wavelength. According to the calculations, a Ge/Al coating with a Ge layer thickness of $d_{1,min} \approx 27$ nm achieves a minimum reflection coefficient of $R_{min} \approx 0.13$ at $\lambda = 800$ nm. For two-layer coatings, the amplitudes of the partial waves in the upper layer depend on the optical constants and thickness of the bottom layer, as can be seen from Eq. 3. Thus, a combination of materials with different extinction coefficients enables the optimal control of the attenuation of waves in the layers of the structure. Consequently, the complete absorption at an arbitrary wavelength from a certain spectral range can be achieved.

It is also important to discuss the angular dependence of the reflection and absorption coefficients of the two-layer structures under consideration. Again, Si/Ge/Al coatings allow unity absorption for any wavelength in the spectral range of 627–1001 nm. Fig. 4 shows the calculated dependence of the absorption coefficient on the angle of incidence θ for different wavelengths in the range of 500–1100 nm. Each horizontal line in Fig. 4 represents a unique coating structure with layer thicknesses $d_{1,min}$ and $d_{2,min}$ corresponding to the first interference minimum of reflection at $\theta = 0$. The blue horizontal lines at 627 nm and 1001 nm correspond to the single-layer Si/Al and Ge/Al coatings, respectively. It can be seen that the angular dependence of the absorption coefficient remains approximately constant in the range of 627–1001 nm.

What affects the choice of materials that constitute a two-layer coating? Consider a coating composed of two different lossy dielectric or semiconducting materials A and B on a substrate from metallic material M . The combination of these layered materials with the substrate material determines two unity absorption wavelengths: $\lambda_0^{A/M}$ and $\lambda_0^{B/M}$. These wavelengths limit the spectral range where the total absorption can be achieved at any wavelength by optimizing the layer thicknesses. Table I provides several examples of various combinations of materials and their corresponding spectral ranges in which the complete absorption of monochromatic radiation can be realized. It can be seen that the considered absorber structures can be designed for visible and near-infrared wavelengths. For example, semiconductors such as Si and SiC can be used in the visible range, whereas Ge and Te are optimal for the near-infrared range. In addition to changing the boundaries of the working spectral range, the choice of materials also affects the absorption pattern inside the layered structure of the coating. Let us consider coatings that combine Si and Ge layers. When using Al as the substrate material for such coatings, up to around 50% (depending on the target wavelength) of the incident radiation can be absorbed by the substrate. Replacing Al with Ag leads to a blue shift in the boundaries of the working spectral range by 80–100 nm. However, in this case, the fraction of radiation absorbed by the substrate drops below 5%. It is also worth noting that an Ag substrate causes lower values of the total optical thickness of the coating. We also note that the proposed two-layer coatings can use a phase-change material as one of the materials of the layers. In this case, the material of the second layer can be selected in such a way as to increase the spectral range in which the actively tunable absorber operates in comparison with a single-layer coating based on this phase-change material.

Another important question is how the antireflective bilayer absorbers proposed in Table 1 might extend the color gamut. A representative way to consider this is to utilize the CIE color specification system. We take Si-Ge-Al and Si-SiC-Al absorber structures as an example. Fig.5 shows the calculated CIE plot for the case of unpolarized normally incident light on Si-Ge-Al (blue dots) and Si-SiC-Al (orange dots) coatings. Each dot on the chromatic diagram corresponds to the optimal layer thicknesses (varying in the range of 0 μ m—40 μm) of the structures, ensuring minimal reflection at any wavelength in the 0.4 μ–1.1 μm region. Fig. 5 demonstrates that use of SiC instead of Ge as a spacer layer increases color purity of the coating. We also calculated the prediction color plot of the Si-Ge-Al (Fig. 6a) and Si-SiC-Al (Fig. 6b) surfaces for a wide range of layers thicknesses. Fig. 6a and Fig. 6b show that the Si-SiC-Al structure provides an increased color contrast, as compared with Si-Ge-Al.

It is also important to comment on the effectiveness of coatings with more than two layers. As shown above, a combination of two materials with different extinction coefficients allows controlling the attenuation of waves in the coating layers. As a result, unity absorption at an arbitrary wavelength from a certain spectral range can be achieved. The addition of a third and subsequent layers is redundant for this purpose. However, the addition of extra layers can be useful for optimizing absorption in a spectral range of a finite width, rather than at a single wavelength.

TABLE I
CALCULATED SPECTRAL RANGES WHERE MONOCHROMATIC TOTAL ABSORPTION CAN BE ACHIEVED FOR VARIOUS COMBINATIONS OF MATERIALS.

Structure	Unity absorption range
Te/Ge/Ag	902–1253 nm
Te/Ge/Au	896–1253 nm
Te/Ge/Al	1001–1298 nm
Te/Ge/Mo	1230–1420 nm
Te/Ge/W	1533–1612 nm
Ge/Si/Ag	546–902 nm
Ge/Si/Au	544–896 nm
Ge/Si/Al	627–1001 nm
Ge/Si/Mo	1005–1230 nm
Ge/Si/W	1361–1533 nm
Si/SiC/Ag	322–546 nm
Si/SiC/Au	503–544 nm
Si/SiC/Al	456–627 nm
Si/SiC/Mo	1004–1005 nm
Si/SiC/W	1239–1361 nm

III. EXPERIMENTAL DEMONSTRATION

For the experimental demonstration of the interference-enhanced absorption in two-layer coatings, we used samples of Si/Ge/Al coatings. The thickness of the lower Ge layer was fixed at 10 nm, and the thickness of the upper Si layer was varied from 15 nm to 30 nm in increments of 5 nm. According to the calculations, in such a range of layer thicknesses, almost complete absorption of the incident radiation around λ = 750 nm could be obtained (see Fig. 2b).

Ge and Si layers were deposited sequentially at room temperature onto an Al substrate layer by physical vapor deposition (electron beam evaporation) in an ultrahigh vacuum environment with a base pressure of typically $1 \cdot 10^{-6}$ Pa or better. A quartz crystal micromass balance (QCM) was used to control the amount of deposited material. In order to translate the QCM mass amount into the layer thickness, grazing incidence X-ray (Cu Kα) reflection was obtained using a Bruker D8 eco for single-layer films in the thickness range of 20–50 nm. The X-ray reflection-determined film thickness results were used to calibrate the QCM.

The optical reflection spectra of the samples were measured using a Bruker IFS 66 v/S Fourier-transform infrared spectrometer. A protected silver mirror (THORLABS PF10-03-P01) was used as the reference sample for the measurements. According to the specification, this mirror guarantees an average reflectance above 97% in the 450–2000 nm wavelength range. The measurements were carried out using an unpolarized radiation beam incident on the surface of a sample at an angle of $11^(o)$ with respect to the surface normal. Fig. 4 shows the measured spectra of the studied Si/Ge/Al coatings. According to our measurements, a structure with a Si layer thickness of 25 nm shows the lowest reflection coefficient $R \approx 0.01$ at $\lambda \approx 850$ nm. The minimum position has a blue shift of about 100 nm with respect to the theoretical prediction. This may be due to differences in the values of the optical constants of the grown Si and Ge layers and the used tabulated optical constants of these materials in the calculations. In any case, our experimental data confirm the possibility of obtaining almost complete absorption of incident radiation by a two-layer coating.

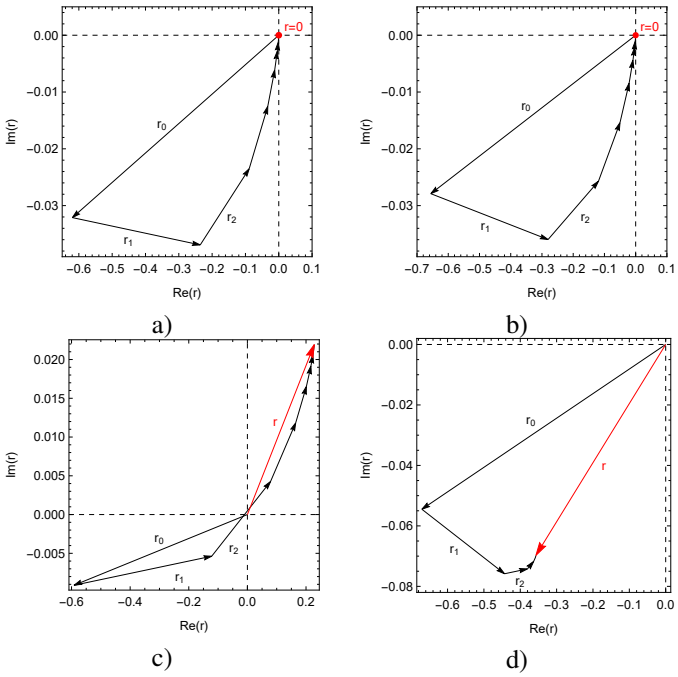

Fig. 3. (a) Calculated phasor diagram for a Si/Al coating optimized for zero reflection at $\lambda = \lambda_0^{Si/Al}$. (b)Calculated phasor diagram for a Ge/Al coating tuned for zero reflection at $\lambda = \lambda_0^{Ge/Al}$. (c) Calculated phasor diagram for a Si/Al coating optimized for the minimum reflection at λ = 800 nm. (d) Calculated phasor diagram for a Ge/Al coating optimized for the minimum reflection at λ = 800 nm.

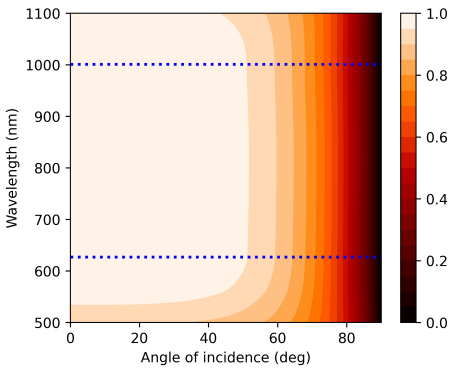

Fig. 4. Calculated dependence R on θ for Si/Ge/Al coatings.

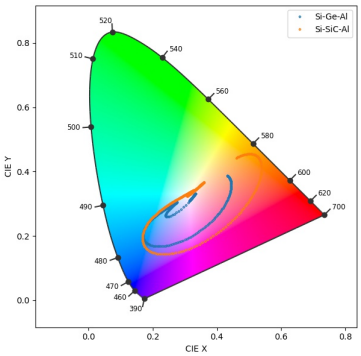

Fig. 5. CIE plot for Si-Ge-Al (blue dots) and Si-SiC-Al (orange dots) structures.

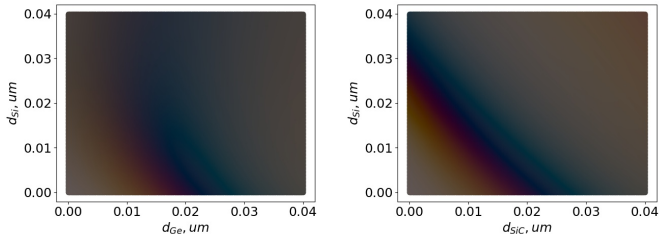

Fig. 6. Calculated color plot of reflective structures (a) Si-Ge-Al and (b) Si-SiC-Al

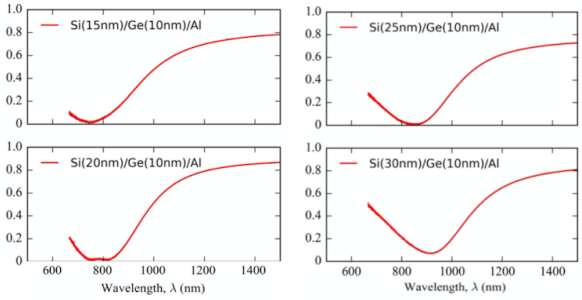

Fig. 7. Measured reflection spectra for Si/Ge/Al coating samples.

IV. Discussion

Let us compare the characteristics of the two-layer coatings considered herein with the solutions proposed earlier [15], [16]. A two-layer coating as well as a single-layer coating on a metasurface substrate provide flexibility in choosing the wavelength at which strong absorption of electromagnetic radiation can be obtained. In this case, the absorption spectra of both types of structures remain fixed during their operation. In contrast, coatings using phase-changing materials enable to control the absorption spectrum during their operation. This is possible because phase-changing materials can be rapidly and reversibly switched between the amorphous and crystalline states by heating. Furthermore, the optical constants (n and κ) of the amorphous and crystalline states differ significantly. A change in the refractive index of the coating material with such a switch between the states allows the position of the interference absorption peak to be shifted. It is important to note that the magnitude of the absorption peak may also change in this case. This happens because when switching between the states, the extinction coefficient also changes and, as a consequence, the optimal matching of the optical constants of the substrate and coating materials can be violated. This effect can be compensated for by using a phase-changing material as a material for one of the coating layers of the structures considered in this work. Moreover, such combination coatings provide more opportunities for the active control of absorption spectra and color gamut.

V. Conclusions

We investigated the absorption of light in two-layer coatings on metal substrates. It is shown that two-layer coatings enable the complete absorption of monochromatic radiation for an arbitrary wavelength from the spectral range, the boundaries of which are determined by a combination of the three materials constituting the structure. It is important to note that the total optical thickness of such a coating remains lower than a quarter of the target wavelength, similar to the case of single-layer coatings. We provided examples of various material combinations that can be used to design light-absorbing coatings for visible and near-infrared radiation. We also experimentally demonstrated the operation principle using Si/Ge/Al coating samples.

References

[1] W. Woltersdorff, "Über die optischen konstanten dünner metallschichten im langwelligen ultrarot," *Zeitschrift für Physik*, vol. 91, no. 3-4, pp. 230–252, 1934.

[2] W. Dallenbach and W. Kleinsteuber, "Reflection and absorption of decimeter-waves by plane dielectric layers," *Hochfreq. u Elektroak*, vol. 51, pp. 152–156, 1938.

[3] K. Park, "The extreme values of reflectivity and the conditions for zero reflection from thin dielectric films on metal," *Applied Optics*, vol. 3, no. 7, pp. 877–881, 1964.

[4] S. Yoshida, "Antireflection coatings on metals for selective solar absorbers," *Thin Solid Films*, vol. 56, no. 3, pp. 321–329, 1979.

[5] R. L. Fante and M. T. McCormack, "Reflection properties of the salisbury screen," *IEEE transactions on antennas and propagation*, vol. 36, no. 10, pp. 1443–1454, 1988.

[6] M. A. Kats, R. Blanchard, P. Genevet, and F. Capasso, "Nanometre optical coatings based on strong interference effects in highly absorbing media," *Nature materials*, vol. 12, no. 1, p. 20, 2013.

[7] H. Deng, Z. Li, L. Stan, D. Rosenmann, D. Czaplewski, J. Gao, and X. Yang, "Broadband perfect absorber based on one ultrathin layer of refractory metal," *Optics letters*, vol. 40, no. 11, pp. 2592–2595, 2015.

[8] S.-T. Yen and P.-K. Chung, "Far-infrared quasi-monochromatic perfect absorption in a thin gaas film on gold," *Optics letters*, vol. 40, no. 16, pp. 3877–3880, 2015.

[9] Z. Li, S. Butun, and K. Aydin, "Large-area, lithography-free super absorbers and color filters at visible frequencies using ultrathin metallic films," *Acs Photonics*, vol. 2, no. 2, pp. 183–188, 2015.

[10] M. A. Kats and F. Capasso, "Optical absorbers based on strong interference in ultra-thin films," *Laser & Photonics Reviews*, vol. 10, no. 5, pp. 735–749, 2016.

[11] J. Rensberg, Y. Zhou, S. Richter, C. Wan, S. Zhang, P. Schöppe, R. Schmidt-Grund, S. Ramanathan, F. Capasso, M. A. Kats, *et al.*, "Epsilon-near-zero substrate engineering for ultrathin-film perfect absorbers," *Physical Review Applied*, vol. 8, no. 1, p. 014009, 2017.

[12] V. Medvedev, V. Gubarev, and C. Lee, "Optical performance of a dielectric-metal-dielectric antireflective absorber structure," *JOSA A*, vol. 35, no. 8, pp. 1450–1456, 2018.

[13] J. Park, J.-H. Kang, A. P. Vasudev, D. T. Schoen, H. Kim, E. Hasman, and M. L. Brongersma, "Omnidirectional near-unity absorption in an ultrathin planar semiconductor layer on a metal substrate," *Acs Photonics*, vol. 1, no. 9, pp. 812–821, 2014.

[14] J. Park, S. J. Kim, and M. L. Brongersma, "Condition for unity absorption in an ultrathin and highly lossy film in a gires–tournois interferometer configuration," *Optics letters*, vol. 40, no. 9, pp. 1960–1963, 2015.

[15] J. Park, J.-H. Kang, S. J. Kim, E. Hasman, and M. L. Brongersma, "Tuning optical absorption in an ultrathin lossy film by use of a metallic metamaterial mirror," *IEEE Photonics Technology Letters*, vol. 27, no. 15, pp. 1617–1620, 2015.

[16] M. A. Kats, D. Sharma, J. Lin, P. Genevet, R. Blanchard, Z. Yang, M. M. Qazilbash, D. Basov, S. Ramanathan, and F. Capasso, "Ultra-thin perfect absorber employing a tunable phase change material," *Applied Physics Letters*, vol. 101, no. 22, p. 221101, 2012.

[17] T. Cao, L. Zhang, R. E. Simpson, and M. J. Cryan, "Mid-infrared tunable polarization-independent perfect absorber using a phase-change metamaterial," *JOSA B*, vol. 30, no. 6, pp. 1580–1585, 2013.

[18] J. K. Behera, K. Liu, M. Lian, and T. Cao, "A reconfigurable hyperbolic metamaterial perfect absorber," *Nanoscale Advances*, vol. 3, no. 6, pp. 1758–1766, 2021.

[19] W. Dong, Y. Qiu, X. Zhou, A. Banas, K. Banas, M. B. Breese, T. Cao, and R. E. Simpson, "Tunable mid-infrared phase-change metasurface," *Advanced Optical Materials*, vol. 6, no. 14, p. 1701346, 2018.

[20] E. D. Palik, *Handbook of optical constants of solids*, vol. 3. Academic press, 1998.
[21] A. D. Rakić, "Algorithm for the determination of intrinsic optical constants of metal films: application to aluminum," *Applied optics*, vol. 34, no. 22, pp. 4755–4767, 1995.
[22] A. Ciesielski, L. Skowronski, W. Pacuski, and T. Szoplik, "Permittivity of ge, te and se thin films in the 200–1500 nm spectral range. predicting the segregation effects in silver," *Materials Science in Semiconductor Processing*, vol. 81, pp. 64–67, 2018.